Solid State Ionics 230 (2013) 43–47

Contents lists available at SciVerse ScienceDirect

Solid State Ionics

journal homepage: www.elsevier.com/locate/ssi

Ab initio calculations of the atomic and electronic structure of $BaZrO_3$ (111) surfaces

R.I. Eglitis *

Institute of Solid State Physics, University of Latvia, 8 Kengaraga Str., Riga LV1063, Latvia

ARTICLE INFO

Article history:
Received 25 May 2012
Received in revised form 29 October 2012
Accepted 31 October 2012
Available online 18 November 2012

Keywords:
Ab initio calculations
(111) surfaces
$BaZrO_3$
B3LYP

ABSTRACT

The paper presents and discusses the results of calculations of surface relaxations and energetics for the polar (111) surface of $BaZrO_3$ using a hybrid B3LYP description of exchange and correlation. On the (111) surface, both Zr- and BaO_3-terminations were analyzed. For both Zr and BaO_3-terminated $BaZrO_3$ (111) surface upper layer atoms, with the sole exception of BaO_3-terminated surface Ba atoms, relax inwards. The Zr-terminated $BaZrO_3$ (111) surface second layer Ba atoms exhibit the strongest relaxation between all Zr and BaO_3-terminated $BaZrO_3$ (111) surface atoms. The calculated surface relaxation energy for Zr-terminated $BaZrO_3$ (111) surface is almost fifteen times larger than the surface relaxation energy for BaO_3-terminated BaZrO3 (111) surface. The surface energy for Zr-terminated $BaZrO_3$ (111) surface (7.94 eV/cell) is smaller, than the surface energy for BaO_3-terminated (111) surface (9.33 eV/cell). The calculated $BaZrO_3$ optical bulk band gap, 4.79 eV is in an excellent agreement with the experimental value, 5.00 eV. The calculated optical band gap for the Zr- and BaO_3-terminated $BaZrO_3$ (111) surfaces becomes smaller with respect to the bulk optical band gap.

1. Introduction

The surfaces of the ABO_3 perovskites are of fundamental interest for basic research as well as important for many industrial applications [1,2]. Motivated by the high fundamental interest and a lot of high technology applications, a substantial amount of theoretical *ab initio* studies dealing with the ABO_3 perovskite (001) and (011) surfaces has been performed during the last quarter of century [3–13].

The experimental and theoretical understanding of ABO_3 perovskites and their surfaces is one of the key topics at the interface between solid state chemistry and solid state physics. During the last years, among all ABO_3 perovskites, experimentally very intensively have been studied the (001) surface of the technologically most important $SrTiO_3$ perovskite. For example, Bickel et al. [14] analyzed the (001) surface structure of $SrTiO_3$ at T = 120 K by means of low-energy-electron diffraction. They got the best theory–experiment fit results for a surface containing domains of two different layer terminations [14]. Four years later, Hikita et al. [15] experimentally studied the electronic and atomic structure of TiO_2 and SrO terminated $SrTiO_3$ (100) surface using reflection high energy electron diffraction (RHEED), XPS and UPS. According to their results, the oxygen atoms on the outermost $SrTiO_3$ surface are pulled out for 0.10 Å and 0.16 Å, respectively [15]. Ikeda et al. [16] determined the surface relaxation and rumpling of TiO_2-terminated $SrTiO_3$ (001) surface by means of medium energy ion scattering (MEIS). Charlton et al. [17] used the X-ray diffraction in order to determine the 300 K structure of $SrTiO_3$ (001) 1×1 with a termination of 78% TiO and 22% of SrO. Their data indicated that a lateral ferroelectric distortion was absent on both terminations [17]. Van der Heide et al. [18] analyzed the chemical and structural properties of several $SrTiO_3$ (001) surfaces prior to and following UHV and O_2 annealing using X-ray photoelectron spectroscopy (XPS), time-of-flight and recoiling spectrometry (TOF-SARS), and low energy electron diffraction (LEED). Their simulations of the TOF-SARS azimuthal scans indicated that the O atoms are located 0.1 Å above the Ti-terminated surface layer [18]. Maus-Friedrichs et al. [19] experimentally investigated the $SrTiO_3$ (001) surface with the metastable impact electron spectra (MIES) and photoelectron spectra (UPS) methods, as well as performed complementary *ab initio* calculations [19]. Finally, Enterkin et al. [20] reported a solution to the 3×1 $SrTiO_3$ (110) surface structure obtained through transmission electron diffraction, and confirmed through density functional theory calculations and scanning tunneling microscopy images and simulations [20].

Taking into account this high technological importance, it is surprising that there have been no *ab initio* studies dealing with the $BaZrO_3$ (111) polar surface. In this study first predictive *ab initio* calculations dealing with atomic and electronic structure of $BaZrO_3$ (111) surface structures are performed. The manuscript is organized as follows. In Section 2 computational details are presented. The results of calculations for surface structures, energies, charge distributions, and band populations are reported in Section 3. Finally, the results are discussed and conclusions are presented in Section 4.

2. Computational details

First-principles DFT–B3LYP calculations have been performed by means of the CRYSTAL computer code [21]. The CRYSTAL code employs Gaussian-type functions (GTF) localized at atoms as the basis for an

* Tel.: +371 67187480.
E-mail address: reglitis@yahoo.com.

0167-2738/$ – see front matter © 2012 Elsevier B.V. All rights reserved.
http://dx.doi.org/10.1016/j.ssi.2012.10.023

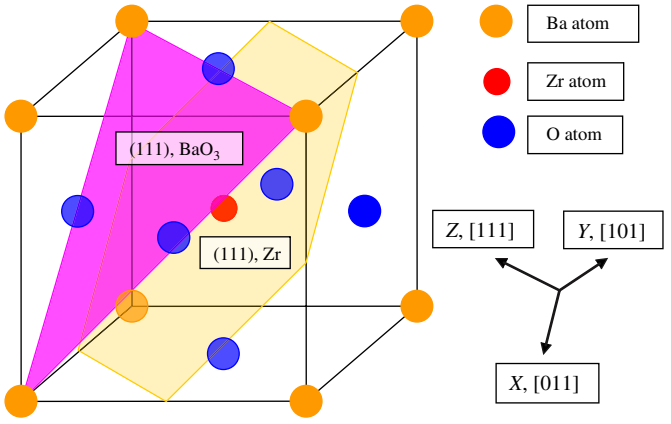

Fig. 1. Sketch of the cubic $BaZrO_3$ perovskite structure showing two possible (111) surface terminations: BaO_3 and Zr.

expansion of the crystalline orbitals. The feature of the CRYSTAL code, which is most important for the study of perovskite surfaces is implementation of the isolated 2D slab model without its artificial repetition along the *z*-axis. However, in order to employ the linear combination of atomic orbitals (LCAO)-GTF method, it is desirable to have optimized basis sets (BS). The optimization of such BS for $SrTiO_3$, $BaTiO_3$ and $PbTiO_3$ perovskites was developed and discussed by Piskunov et al. [22]. In the present paper, for O atoms, this new BS which differs from the previous calculations [23,24] by inclusion of polarisable *d*-orbitals on O ions was used. For Ba and Zr atoms the same basis set as in Refs. [12,13] was used. In order to avoid charged supercells in calculations, 2 electrons have been added to Ba^{2+} ion, 4 electrons to Zr^{4+} ion, and 2 electrons were removed from the O^{2-} ion. Thereby all $BaZrO_3$ (111) surface calculations were performed using neutral Ba, Zr and O atoms, and, of course, also neutral slabs containing 21 or 24 atoms, respectively.

All calculations have been performed using the hybrid exchange–correlation B3LYP functional involving a hybrid of nonlocal Fock exact exchange, LDA exchange and Becke's gradient corrected exchange functional [25], combined with the nonlocal gradient corrected correlation potential by Lee–Yang–Parr [26]. The Hay–Wadt small-core effective core pseudopotentials (ECPs) have been adopted for Ba

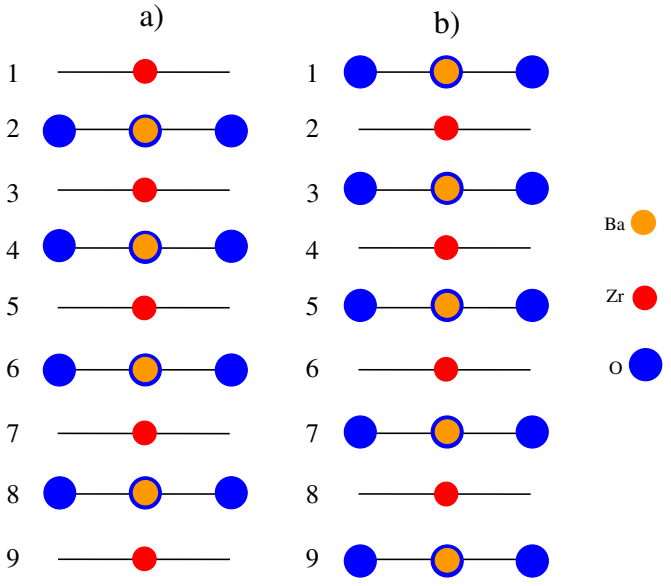

Fig. 2. Sketch of the side views of slab geometries used to study $BaZrO_3$ (111) surfaces. (a) Non-stoichiometric nine-layer slab with Zr-terminated surfaces. (b) Non-stoichiometric nine-layer slab with BaO_3-terminated surfaces.

Table 1
The calculated lattice constant (in Å) for the $BaZrO_3$ bulk using the hybrid B3LYP method. The experimental bulk lattice constant [35] is listed for comparison.

Material	Calculated lattice constant	Experim. lattice constant
$BaZrO_3$	4.234	4.192

and Zr atoms [27,28]. The small-core ECPs replace only inner core orbitals, but orbitals for sub-valence electrons as well as for valence electrons are calculated self-consistently. Light oxygen atoms have been treated with the all-electron BS [22].

The reciprocal space integration has been performed by sampling the Brillouin zone of the five-atom cubic unit cell with the $5\times5\times1$ Pack–Monkhorst net [29] that provides the balanced summation in direct and reciprocal spaces. To achieve high accuracy, large enough tolerances of 7, 8, 7, 7, and 14 have been chosen for the Coulomb overlap, Coulomb penetration, exchange overlap, the first exchange pseudo-overlap, and for the second exchange pseudo-overlap, respectively [21].

The $BaZrO_3$ (111) surfaces have been modeled with two-dimensional (2D) slabs, consisting of nine planes perpendicular to the [111] crystal direction. To simulate $BaZrO_3$ (111) surfaces, symmetrical (with respect to the mirror plane) slabs consisting of nine alternating Zr and BaO_3 layers were used. One of these slabs is terminated by Zr planes and consists of a supercell containing 21 atoms (Zr–BaO_3–Zr–BaO_3–Zr–BaO_3–Zr–BaO_3–Zr) (see Fig. 2a). The second slab is terminated by BaO_3 planes and consists of a supercell containing 24 atoms (BaO_3–Zr–BaO_3–Zr–BaO_3–Zr–BaO_3–Zr–BaO_3) (see Fig. 2b). These slabs are non-stoichiometric, with unit cell formulas $Ba_4Zr_5O_{12}$ and $Ba_5Zr_4O_{15}$, respectively (see Fig. 1). As it is well known from previous studies dealing with polar $CaTiO_3$ and $SrTiO_3$ (111) surfaces [30–34], a strong electron redistribution takes place for such terminations in order to cancel the polarity, but the Zr or BaO_3-terminated $BaZrO_3$ (111) surface keeps its insulating character, and such calculations are feasible. Of course, it is not possible to perform calculations for asymmetric slabs with different terminations, for example, Zr–BaO_3–Zr–BaO_3–Zr–BaO_3–Zr–BaO_3, since this would lead to a large dipole moment for an asymmetric slab.

The second well established approach for ABO_3 perovskite polar (111) surface calculations, which was not used in the present paper, is artificial modification of surface structure by removing O atoms from the BaO_3-terminated $BaZrO_3$ (111) surface and adding O atoms onto the Zr-terminated surface, respectively. Such surface structure changes, (BaO_2–Zr–BaO_3–Zr–BaO_3–Zr–BaO_3–Zr–BaO_2) or (ZrO–BaO_3–Zr–BaO_3–Zr–BaO_3–Zr–BaO3–ZrO) can, in principle, provide the polarity compensation and calculations for such artificially neutral $BaZrO_3$ (111) surfaces also may be feasible.

As a next step, the cleavage and surface energies were calculated. It is obvious that Zr and BaO_3-terminated (111) surfaces are mutually complementary. Surfaces with both terminations arise simultaneously under cleavage of the crystal and the relevant cleavage energy is distributed equally between created surfaces. Therefore, it is assumed that the cleavage energy is the same for both terminations. The cleavage energy of the complementary surface $E_{cl}(BaO_3+Zr)$ can be obtained from the

Table 2
Calculated effective charges *Q* and bond populations *P* (in *e*) for bulk $BaZrO_3$.

$BaZrO_3$		
Ion or bond	Property	Value
Ba	*Q*	+1.810
O	*Q*	−1.319
Zr	*Q*	+2.146
Ba-O	*P*	−0.012
Zr-O	*P*	+0.106
O-O	*P*	−0.008

Table 3
Calculated relaxation of Zr-terminated $BaZrO_3$ (111) surface upper three layer atoms (as a percentage of the bulk crystal lattice constant a = 4.234 Å). Positive (negative) values refer to displacements in the direction outwards (inwards) the surface.

Layer	Ion	Displacement (Δz)
1	Zr	−8.03
2	Ba	−9.73
	O	+0.78
3	Zr	−0.02

total energies computed for the unrelaxed slabs through the following equation:

$$E_{cl}(BaO_3 + Zr) = {}^1/_4\left[E_{slab}{}^{unrel}(Zr) + E_{slab}{}^{unrel}(BaO_3) - 9E_{bulk}\right] \quad (1)$$

where $E_{slab}^{unrel}(Zr)$ is the total energy of unrelaxed 21-atom Zr-terminated slab, according to B3LYP calculations performed in the framework of this paper equal to −33696.3767 eV (see Fig. 2a). The total energy of unrelaxed 24-atom BaO_3-terminated $BaZrO_3$ (111) slab $E_{slab}^{unrel}(BaO_3)$ is equal to −39261.0788 eV (see Fig. 2b). E_{bulk} is the bulk energy per formula unit containing 5 atoms in the cubic $BaZrO_3$ structure, and according to performed calculations equal to −8110.5757 eV. Factor 9 in Eq. (1) before the E_{bulk} comes from the fact that 21-atom Zr-terminated and 24-atom BaO_3-terminated $BaZrO_3$ (111) slabs together contain nine 5-atom $BaZrO_3$ bulk unit cells. Factor ¼ means that totally four surfaces (upper and lower surfaces for Zr and BaO_3-terminated $BaZrO_3$ (111) surfaces, as depicted in Fig. 2) are created upon the crystal cleavage.

When both sides of the slab are allowed to relax, the relaxation energies for each of the surfaces can be obtained by the equation:

$$E_{rel}(\lambda) = {}^1/_2\left[E_{slab}{}^{rel}(\lambda) - E_{slab}{}^{unrel}(\lambda)\right] \quad (2)$$

where λ = Zr or BaO_3 specifies the $BaZrO_3$ (111) termination. E_{slab}^{rel} (Zr) is the Zr-terminated slab energy after relaxation, equal to −33699.3539 eV and $E_{slab}^{rel}(BaO_3)$ is the BaO_3-terminated slab energy after geometry relaxation equal to −39261.2791 eV. Factor ½ means that two surfaces are created upon the crystal cleavage (upper and lower surfaces of Zr-terminated $BaZrO_3$ (111) surface, or upper and lower surfaces of BaO_3-terminated $BaZrO_3$ (111) surface, respectively, as depicted in Fig. 2). Now when the cleavage and relaxation energies are calculated, the surface energy is just a sum of them:

$$E_{surf}(\lambda) = E_{cl}(BaO_3 + Zr) + E_{rel}(\lambda). \quad (3)$$

3. Main results

As a starting point of the calculations, the $BaZrO_3$ bulk lattice constant has been calculated. The calculated bulk lattice constant for $BaZrO_3$ (4.234 Å) is slightly larger than the experimental value of 4.192 Å [35] (see Table 1). Thus, the computational approach used in the present study can be established as appropriate. The theoretical $BaZrO_3$ bulk lattice constant was used in the following $BaZrO_3$ polar (111) surface structure calculations.

Table 4
Calculated relaxation of BaO_3-terminated $BaZrO_3$ (111) surface upper three layer atoms (as a percentage of the bulk crystal lattice constant a = 4.234 Å).

Layer	Ion	Displacement (Δz)
1	Ba	+1.70
	O	−0.57
2	Zr	+0.21
3	Ba	+0.71
	O	−0.01

Table 5
Calculated cleavage, relaxation, and surface energies for $BaZrO_3$ (111) surfaces (in electron volt per surface cell).

Surface	$E_{cl}(BaO_3 + Zr)$	Termination	$E_{(rel)}$	$E_{(surf)}$
$BaZrO_3$ (111)	9.43	Zr-term.	−1.49	7.94
		BaO_3-term.	−0.10	9.33

The effective Mulliken [36] charges for Ba atom (+1.810*e*) (see Table 2), calculated by means of B3LYP method, are approximately by 10% smaller than the classical ionic charges (+2*e*) widely used in the shell model calculations. Calculated effective charges for the Zr atom (+2.146*e*) and for the O atom (−1.319e) are considerably smaller than the standard ionic charges (+4*e* and −2*e*, respectively) indicating a large amount of covalency in the chemical bonding between Zr and O atoms. The covalent nature of the chemical bonding between Zr and O atoms is confirmed also by the large bond population value between Zr and O atoms (+0.106*e*). The bond population value of (−0.012*e*) between Ba and O atoms is typical also for another previously studied ABO_3 perovskites, such as for example $SrTiO_3$, $BaTiO_3$, $PbTiO_3$ and $CaTiO_3$ [4,9,11].

According to the results of calculations, the upper layer Zr atom for Zr-terminated $BaZrO_3$ (111) surface strongly (by 8.03% of bulk lattice constant a_o) relaxes inwards towards the bulk (see Table 3). The second layer Ba atom relaxes inwards even more strongly (by 9.73% of a_o), while the second layer O atom relaxes slightly outwards by 0.78% of a_o. Inward relaxation of the third layer Zr atom is very weak, only 0.02% of a_o.

For BaO_3-terminated $BaZrO_3$ (111) surface the upper layer metal and oxygen atoms relax outwards and inwards by 1.70% of a_o and 0.57% of a_o, respectively (see Table 4). The second layer Zr atom outward relaxation magnitude (0.21% of a_o) is smaller than the third layer metal atom displacement magnitude. Third layer Ba atoms relax outwards (0.71% of a_o), while the third layer O atoms relax inwards by a very small magnitude (0.01% of a_o).

The calculated surface relaxation energy for Zr-terminated $BaZrO_3$ (111) surface (−1.49 eV) is almost fifteen times larger than the surface relaxation energy for BaO_3-terminated $BaZrO_3$ (111) surface (−0.10 eV) (see Table 5). The calculated surface energy for Zr-terminated $BaZrO_3$ (111) surface is equal to (7.94 eV/cell), while the surface energy for BaO_3-terminated $BaZrO_3$ (111) surface is equal to (9.33 eV/cell).

The discussion of the electronic structure of Zr- and BaO_3-terminated $aZrO_3$ (111) surfaces begins with the analysis of charge redistribution in near-surface planes. The calculated atomic displacements, effective static atomic charges (calculated using Mulliken population analysis) and bond populations between nearest metal and oxygen atoms are presented in Tables 6 and 7. A strong electron redistribution takes place near the

Table 6
Calculated absolute magnitudes of atomic displacements *D* (in Å), the effective atomic charges *Q* (in *e*) and the bond populations *P* between nearest Me and O atoms (in *e*) for the Zr-terminated $BaZrO_3$ (111) surface. Positive (negative) values refer to displacements in the direction outwards (inwards) the surface.

Zr-terminated $BaZrO_3$ (111) surface			
Layer	Property	Ion	Value
1	*D*	Zr	−0.34
	Q		+1.462
	P		+0.002
2	*D*	Ba	−0.412
	Q		+1.715
	P		−0.004
	D	O	+0.033
	Q		−1.287
	P		+0.098
3	*D*	Zr	−0.001
	Q		+1.965
	P		+0.002

Table 7
Calculated absolute magnitudes of atomic displacements D (in Å), the effective atomic charges Q (in e) and the bond populations P between nearest Me and O atoms (in e) for the BaO_3-terminated $BaZrO_3$ (111) surface. Positive (negative) values refer to displacements in the direction outwards (inwards) the surface.

BaO_3-terminated $BaZrO_3$ (111) surface			
Layer	Property	Ion	Value
1	D	Ba	+0.072
	Q		+1.828
	P		−0.006
	D	O	−0.024
	Q		−0.983
	P		+0.118
2	D	Zr	+0.009
	Q		+2.159
	P		−0.002
3	D	Ba	+0.030
	Q		+1.804
	P		−0.012
	D	O	0
	Q		−1.311
	P		+0.104

upper surface layers, but both Zr- and BaO_3-terminated (111) surfaces keep its insulating character. Table 6 shows that calculated Mulliken effective charge Q for the Zr-terminated $BaZrO_3$ (111) surface upper layer Zr atom (+1.462e) is very strongly by 0.684e reduced with respect to bulk $BaZrO_3$ value (+2.146e). Metal atoms in the second and third layers lose much less charge, with Ba and Zr atoms losing 0.095e and 0.181e, respectively. The O atoms in the second layer have charges that are only slightly reduced by 0.032e (i. e., they become less negative).

First of all, note in Table 7 that the effective static charges of Ba (+1.828e) on the BaO_3-terminated $BaZrO_3$ (111) surface are close to the +2e formal ionic charges, whereas that of O (−0.983e) is considerably smaller. Metal atoms in the first and second layers gain some very small additional charge (0.018e and 0.013e) with respect to bulk $BaZrO_3$. In contrast, the O atoms in the first layer have charges that are very strongly by 0.336e reduced (*i.e.*, they become less negative). The Zr−O bond populations between the first and second layers (+0.118e) for the BaO_3-terminated BaZrO3 (111) surface are approximately 10% larger than the relevant Zr−O bond population in the $BaZrO_3$ bulk (+0.106e). Between deeper layers, for example, between the third and fourth layers for BaO_3-terminated $BaZrO_3$ (111) surface the Zr-O bond population already becomes very close (+0.104e) to the $BaZrO_3$ bulk bond population value. In contrast, all possible O−O bond populations, which are not shown in Tables 6 and 7, are negative, which indicates the repulsion between O and O atoms.

By means of the hybrid B3LYP method calculated optical band gap for $BaZrO_3$ bulk (4.79 eV) is in an outstanding agreement with the experimental value of (5.00 eV) [37]. This is not a trivial achievement, since it is a well-known fact that DFT–LDA calculations strongly underestimate the optical band gap. On the other hand, the optical band gap value obtained through pure-HF calculations usually greatly overestimates the experimental band gap value. As it is typical for ABO_3 perovskites [13,24], the calculated optical band gap for $BaZrO_3$ (111) surfaces becomes smaller with respect to the bulk optical band gap. The B3LYP calculated $BaZrO_3$ (111) surface optical band gaps are approximately by 6% reduced with respect to the $BaZrO_3$ bulk optical band gap value and are equal to (4.47 eV) for the Zr-terminated surface, and (4.51 eV) for the BaO_3-terminated $BaZrO_3$ (111) surface (see Table 8).

4. Conclusions

By means of the hybrid B3LYP approach, the Zr- and BaO_3-terminated $BaZrO_3$ polar (111) surface relaxations have been calculated. For both Zr- and BaO_3-terminated $BaZrO_3$ (111) surfaces the upper layer atoms, with the sole exception of the BaO_3-terminated surface Ba atoms, relax inwards. The second layer atoms for both (111) surfaces, with the exception of Zr-terminated $BaZrO_3$ (111) surface Ba atoms, relax outwards. All third layer atoms on the Zr- and BaO_3-terminated $BaZrO_3$ (111) surfaces, with the exception of third layer Ba atoms, relax inwards. The Zr-terminated $BaZrO_3$ (111) surface second layer Ba atoms exhibit the strongest relaxation between all Zr and BaO_3-terminated $BaZrO_3$ (111) surface atoms.

Table 8
Calculated optical band gap for the BaO_3- and Zr-terminated $BaZrO_3$ (111) surfaces (in eV). Experimental value [37] is listed for comparison.

Termination	$BaZrO_3$ optical band gap
Bulk	4.79
BaO_3-terminated $BaZrO_3$ (111) surface	4.51
Zr-terminated $BaZrO_3$ (111) surface	4.47
Experiment [37]	5.00

The calculated surface relaxation energy for Zr-terminated $BaZrO_3$ (111) surface is almost fifteen times larger than the surface relaxation energy for BaO_3-terminated $BaZrO_3$ (111) surface. The surface energy for Zr-terminated $BaZrO_3$ (111) surface (7.94 eV/cell) is smaller than the surface energy for BaO_3-terminated (111) surface (9.33 eV/cell).

The polar $BaZrO_3$ (111) surfaces have the largest surface energies (7.94 eV/cell) and (9.33 eV/cell) between all possible $BaZrO_3$ surface terminations, and thereby they are the less energetically stable $BaZrO_3$ surfaces. The most energetically favorable, according to related B3LYP calculations performed in Ref. [12], are the neutral BaO (1.30 eV/cell) and ZrO_2 (1.31 eV/cell) terminated $BaZrO_3$ (001) surfaces. The Ba (2.90 eV/cell), ZrO (3.09 eV/cell) and O (2.32 eV/cell) terminated $BaZrO_3$ polar (011) surfaces are by a factor of approximately 2 less stable than the $BaZrO_3$ (001) surfaces [12], but by a factor of around 3 more stable than the $BaZrO_3$ (111) surfaces.

By means of the B3LYP method calculated $BaZrO_3$ optical bulk band gap (4.79 eV) is by only approximately 4% underestimated regarding the experimental value of (5.00 eV). The calculated optical band gap near the Zr- and BaO_3-terminated $BaZrO_3$ surfaces is by approximately 6% reduced with respect to the bulk value. The B3LYP calculated optical band gap values for Zr- and BaO_3-terminated $BaZrO_3$ (111) surfaces are very close, and differ only by 0.04 eV.

Acknowledgments

The present work was supported by ESF grant no. 2009/0202/1DP/1.1.1.2.0/09/APIA/VIAA/141.

References

[1] J.F. Scott, Ferroelectric Memories, Springer, Berlin, 2000.
[2] M.E. Lines, A.M. Glass, Principles and Applications of Ferroelectrics and Related Materials, Clarendon, Oxford, 1977.
[3] N. Erdman, K.R. Poeppelmeier, M. Asta, O. Warschkow, D.E. Ellis, L.D. Marks, Nature 419 (2002) 55.
[4] R.I. Eglitis, D. Vanderbilt, Phys. Rev. B 77 (2008) 195408.
[5] E.A. Kotomin, R.I. Eglitis, J. Maier, E. Heifets, Thin Solid Films 400 (2001) 76.
[6] A. Hofer, M. Fechner, K. Duncker, M. Holzer, I. Mertig, W. Widdra, Phys. Rev. Lett. 108 (2012) 087602.
[7] R.I. Eglitis, G. Borstel, E. Heifets, S. Piskunov, E. Kotomin, J. Electroceram. 16 (2006) 289.
[8] M. Stengel, Phys. Rev. B 84 (2011) 205432.
[9] R.I. Eglitis, D. Vanderbilt, Phys. Rev. B 78 (2008) 155420.
[10] A.M. Kolpak, D. Li, R. Shao, A.M. Rappe, D.A. Bonnell, Phys. Rev. Lett. 101 (2008) 036102.
[11] R.I. Eglitis, D. Vanderbilt, Phys. Rev. B 76 (2007) 155439.
[12] R.I. Eglitis, J. Phys. Condens. Matter 19 (2007) 356004.
[13] R.I. Eglitis, M. Rohlfing, J. Phys. Condens. Matter 22 (2010) 415901.
[14] N. Bickel, G. Schmidt, K. Heinz, K. Müller, Phys. Rev. Lett. 62 (1989) 2009.
[15] T. Hikita, T. Hanada, M. Kudo, M. Kawai, Surf. Sci. 287–288 (1993) 377.
[16] A. Ikeda, T. Nishimura, T. Morishita, Y. Kido, Surf. Sci. 433–435 (1999) 520.
[17] G. Charlton, S. Brennan, C.A. Muryn, R. McGrath, D. Norman, T.S. Turner, G. Thorthon, Surf. Sci. 457 (2000) L376.

[18] P.A.W. Van der Heide, Q.D. Jiang, Y.S. Kim, J.W. Rabalais, Surf. Sci. 473 (2001) 59.
[19] W. Maus-Friedrichs, M. Frerichs, A. Gunhold, S. Krischok, V. Kempter, G. Bihlmayer, Surf. Sci. 515 (2002) 499.
[20] J.A. Enterkin, A.K. Subramanian, B.C. Russel, M.R. Castell, K.R. Poeppelmeier, L.D. Marks, Nat. Mater. 9 (2010) 245.
[21] V.R. Saunders, R. Dovesi, C. Roetti, M. Causa, N.M. Harrison, R. Orlando, C.M. Zicovich- Wilson, CRYSTAL-2006 User Manual, University of Torino, Torino, Italy, 2006.
[22] S. Piskunov, E. Heifets, R.I. Eglitis, G. Borstel, Comput. Mater. Sci. 29 (2004) 165.
[23] E. Heifets, R.I. Eglitis, E.A. Kotomin, J. Maier, G. Borstel, Phys. Rev. B. 64 (2001) 235417.
[24] E. Heifets, R.I. Eglitis, E.A. Kotomin, J. Maier, G. Borstel, Surf. Sci. 513 (2002) 211.
[25] A.B. Becke, J. Chem. Phys. 98 (1993) 5648.
[26] C. Lee, W. Yang, R.G. Parr, Phys. Rev. B 37 (1988) 785.
[27] P.J. Hay, W.R. Wadt, J. Chem. Phys. 82 (1985) 299.
[28] W.R. Wadt, P.J. Hay, J. Chem. Phys. 82 (1985) 284.
[29] H.J. Monkhorst, J.D. Pack, Phys. Rev. B 13 (1976) 5188.
[30] W. Liu, C. Wang, J. Cui, Z.Y. Man, Solid State Commun. 149 (2009) 1871.
[31] R.I. Eglitis, Ferroelectrics 424 (2011) 1.
[32] R.I. Eglitis, M. Rohlfing, Phys. Stat. Solidi B, in press http://dx.doi.org/10.1002/pssb.201248072.
[33] A. Pojani, F. Finocchi, C. Noguera, Surf. Sci. 442 (1999) 179.
[34] A. Pojani, F. Finochi, C. Noguera, Appl. Surf. Sci. 142 (1999) 177.
[35] J.W. Bennett, I. Grinberg, A.M. Rappe, Phys. Rev. B 73 (2006) (180102(R)).
[36] C.R.A. Catlow, A.M. Stoneham, J. Phys. C: Solid State Phys. 16 (1983) 4321.
[37] O. Fursenko, J. Bauer, G. Lupina, P. Dudek, M. Lukosius, C. Wenger, P. Zaumseil, Thin Solid Films 520 (2012) 4532.